## Research Article

# The size of the Greenland Ice Sheet during Marine Isotope Stage 3

Jason Briner[a], Darrell Kaufman[b] and Ole Bennike[c]

[a]Department of Geology, University at Buffalo, Buffalo, NY 14221, USA; [b]School of Earth and Sustainability, Northern Arizona University, Flagstaff, AZ, USA and [c]Geological Survey of Denmark and Greenland, DK-1350 Copenhagen K, Denmark

## Abstract

Ice-sheet volume during Marine Isotope Stage (MIS) 3 (57–29 ka) is controversial. Several recent studies have proposed that the Greenland Ice Sheet was smaller during MIS 3 than it is today based on radiocarbon ages of molluscan bivalve shells reworked into sedimentary deposits adjacent to the present ice margin. Such a result contrasts with available records of MIS 3 climate, ice volume, and sea level. We revisited a site previously interpreted as containing evidence for smaller than present ice during MIS 3. We collected marine bivalve shells and combined progressive acid dissolution in preparation for radiocarbon dating with new-generation amino acid analysis, which focuses on aspartic acid racemization. Our results suggest that contamination by young carbon yields finite radiocarbon ages despite bivalve shells likely dating to MIS 5e (∼125 ka) or even older. This result should be further tested, which could be accomplished with additional studies of this kind in combination with ice-sheet modeling and additional paleoclimate data generated from adjacent seas.

**Keywords:** Greenland Ice Sheet; Marine Isotope Stage 3; Radiocarbon Dating; Amino Acid Geochronology

## INTRODUCTION

Glacial–interglacial cycles, oscillations of ice sheets, and global sea level are the defining feature of the Quaternary Period. The pattern and pace of changes in global ice volume in response to climate forcings during the last glacial period are of particular relevance to the ongoing societal challenge of ice loss and sea-level rise (Tierney et al., 2020; Fox-Kemper et al., 2021). However, deconvolving globally integrated records of ice volume from far-field sea-level records or from the benthic $\delta^{18}O$ stack into volume changes of specific ice sheets is not straightforward (Lisiecki and Raymo, 2005; Clark et al., 2024). Doing so requires field observations of past changes of individual ice sheets, for which the geologic record remains incomplete (e.g., Batchelor et al., 2019). Likewise, there are gaps in knowledge on sea-level high stands during recent interglaciations like Marine Isotope Stage (MIS) 5e (∼125 ka; Kopp et al., 2013; Dumitru et al., 2023) and intermediate climate periods like MIS 3 (57–29 ka; e.g., Lisiecki and Raymo, 2005; Dalton et al., 2022; Farmer et al., 2023). The size of Northern Hemisphere ice sheets during MIS 3 is controversial. It seems that the Fennoscandian Ice Sheet completely deglaciated during MIS 3 (e.g., Mangerud et al., 2008, 2023), whereas the larger Laurentide Ice Sheet survived MIS 3. However, there are various depictions of Laurentide Ice Sheet size during MIS 3 (Gowan et al., 2021; Batchelor et al., 2019). Based on interpretations of a large data compilation and their earlier work in the Hudson lowlands, Dalton et al. (2019) suggested that Hudson Bay, near the center of the Laurentide Ice Sheet, was ice-free for parts of MIS 3. Some recent sea-level reconstructions

and reassessments would be consistent with such a decrease in Laurentide Ice Sheet volume (e.g., Pico et al., 2017). On the other hand, scrutiny of field data and radiocarbon ages as well as luminescence chronologies has led other authors to suggest continuous ice cover over Hudson Bay through MIS 3 (Miller and Andrews, 2019; Hodder et al., 2023). This controversy in part stems from the challenging nature of interpreting radiocarbon ages close to the limit of the radiocarbon dating method.

Recent work has also concluded that the Greenland Ice Sheet was smaller than it is at present during late MIS 3 (Larsen et al., 2018, 2019; Søndergaard et al., 2019). This is unexpected, because a variety of evidence for global ice volume and sea level indicates that ice-sheet volume during MIS 3 was significantly greater than during the Holocene. The conclusion of a Holocene-sized ice sheet during MIS 3 is based on finite radiocarbon ages of marine bivalve shells eroded by overriding ice flow from offshore to onshore and redeposited into till in areas near the present ice margin. In some cases, such bivalve shells were found in recently deposited (historical) moraines (Larsen et al., 2019), and in other cases, they were found in till slightly beyond the historical ice limit (Weidick et al., 1996; Larsen et al., 2018; Søndergaard et al., 2019). Because the shells represent marine species from sites that are now covered by the ice sheet, the finds require that the ice sheet was smaller than at present during MIS 3, if the ages are correct.

Because such a history would be at odds with our understanding of Greenland Ice Sheet size inferred from global ice-volume records, these recent interpretations require attention. Such scrutiny is particularly important given prior work showing that minor contamination by young carbon can cause bivalve shells that are actually older than the range of radiocarbon dating (>50 ka) to return finite ages that fall within MIS 3 (e.g., Bednarski, 1995; Busschers et al., 2014). We revisited a site described by

Weidick et al. ([1996](#)) with reported MIS 3 bivalve ages from till adjacent to Storstrømmen in NE Greenland ([Fig. 1](#)). We measured radiocarbon in Holocene and pre-Holocene shells subjected to progressive acid dissolution. Furthermore, we measured the extent of amino acid racemization (AAR) in our Holocene and pre-Holocene shells from Storstrømmen and compared these with new measurements on shells in East Greenland previously collected from MIS 5 (the last interglacial) deposits. While the exchange of inorganic carbon between a shell and its surrounding environment influences its $^{14}$C age, this process does not influence the amino acids.

## STUDY SITE AND METHODS

Storstrømmen is the southernmost outlet glacier complex draining the NE Greenland ice stream ([Fig. 1](#)). Sub–ice sheet topography shows Storstrømmen flowing through a strait with a floor ∼400 m below sea level (Morlighem et al., [2017](#)). Weidick et al. ([1996](#)) hypothesized that Storstrømmen retreated out of this strait after ∼8 ka, during the latest stages of the last deglaciation. This was followed by an advance back to its present configuration in the Late Holocene, based on bivalve shells reworked into the historical moraine along the ice margin ([Fig. 1](#)). Confirming this general timing are previously published radiocarbon ages from these shells dating to the Middle and Late Holocene (Weidick et al., [1996](#); Supplementary Table 1). Additionally, Weidick et al. ([1996](#)) obtained radiocarbon ages of shells found in till that drapes the terrain beyond the historical moraine. From four different locations, these shells yielded nonfinite radiocarbon ages (>40,000 $^{14}$C yr BP, n = 4). One of the localities also yielded finite ages (∼33,300 to ∼24,900 $^{14}$C yr BP, n = 4).

In summer 2023, we re-collected whole and fragmented bivalve shells (none articulated) from the site where Weidick et al. ([1996](#)) reported finite ages (77.14211°N, 21.95788°W). Here, at site 23GRØm-06, till drapes the landscape and bivalves are found where streams and wind are eroding the surface. Additionally, we collected bivalves from historical moraines at two locations, one adjacent to the till collection site (23GRØm-09; 77.14175°N, 21.98706°W), and one near the terminus of Storstrømmen (23GRØm-12; 76.87546°N, 22.41031°W; [Fig. 1](#)). We selected 10 shells of *Mya truncata* from each of our three sites for amino acid analysis plus 3 *Hiatella arctica* and 4 *Astarte borealis* shells from till. For radiocarbon dating, we selected four *Mya truncata* and two *Astarte borealis* shell fragments from the till site and two *Mya truncata* fragments from site 23GRØm-12.

In addition to collecting new field samples, we also obtained archived *Mya truncata* bivalve fragments for new amino acid analysis. The samples were collected in the early 1990s from stratigraphic sections in the Langelandselv area of Jameson Land, East Greenland. Based on luminescence chronology, stratigraphic relationships, relative sea-level interpretations, and the presence of thermophilic, southern extralimital species, the stratigraphic units were assigned to MIS 5e (Bennike and Böcher, [1994](#); Landvik et al., [1994](#); Vosgerau et al., [1994](#)). We analyzed nine fragments from two different MIS 5e sample sites (Supplementary Table 2).

### AAR methods

Shells were prepared for amino acid analysis according to standard procedure (Wehmiller and Miller, [2000](#)). First, they were cleaned by mechanical grinding and acid leaching. The total hydrolyzable amino acid population was analyzed by demineralizing the shells in 20 μL of 7 M HCl per mg of $CaCO_3$ then hydrolyzing

under $N_2$ at 110°C for 22 h. Sample solutions were evaporated to dryness *in vacuo* and rehydrated in 0.01 M HCl containing an internal standard of L-*homo*-arginine. The chromatographic instrumentation and procedure used to separate amino acid enantiomers is presented by Kaufman and Manley ([1998](#)). Briefly, the analytical method employed pre-column derivatization with *o*-phthaldialdehyde together with the chiral thiol, *N*-isobutyryl-L-cysteine, to yield fluorescent diastereomeric derivatives of chiral (D and L) amino acids. The derivatization was performed online before each injection using the auto-injector of an integrated Agilent 1100 high-performance liquid chromatograph. Separation was by a reverse-phase column packed with a $C_{18}$ stationary phase using a linear gradient of aqueous sodium acetate, methanol, and acetonitrile. Detection was by fluorescence. The average analytical uncertainty (internal reproducibility) measured by the coefficient of variation for multiple injections of laboratory standards was typically between 3% and 5% for the D/L values of most of the amino acids. Interlaboratory comparison standards (Wehmiller, [1984](#)) were analyzed along with each batch of unknowns.

### Radiocarbon dating methods

Previous studies have shown that shells and corals contaminated by young carbon exhibit progressively less contamination (older ages) inward from the specimen's margin (Burr et al., [1992](#); Hajdas et al., [2004](#); Bard et al., [2015](#)). However, a more recent study based on three molluscan taxa showed mixed response to stepwise dissolution (Busschers et al., [2014](#)). To test for contamination of potential radiocarbon-dead shells, we performed differential dissolution of shell subsamples by removing 10%, 50%, and 90% of the shell mass using 2 M HCl before radiocarbon dating. Each shell was broken into subpieces, all near the umbo (hinge area) where the shell is thickest. One piece was used for amino acid analysis, and three were used for radiocarbon dating. Radiocarbon was measured on a MIni CArbon DAting System (MICADAS) (Synal et al., [2007](#)) in the Arizona Climate and Ecosystems (ACE) Isotope Laboratory at Northern Arizona University. All shells from the till site and one from an historical moraine were converted to graphite using the Automated Graphitization Equipment (AGE3, IonPlus), which employs an elemental analyzer to combust the organic and inorganic shell carbon. Because analytical precision for Holocene shells is less critical, rather than making graphite targets, we used the Carbonate Handling System (CHS), which acidifies the inorganic carbon and injects the evolved $CO_2$ directly into the Gas Ion Source (GIS) of the MICADAS (Wacker et al., [2013](#)). The performance of the MICADAS in the ACE Lab for biocarbonates is documented by Bright et al. ([2024](#)).

## RESULTS

All radiocarbon ages from the till site (23GRØm-06) are finite. The ages of *Mya* shell subsamples with 10% of the outer mass removed by acid dissolution range from 35,130 ± 150 to 24,210 ± 60 $^{14}$C yr BP ([Fig. 2](#); [Table 1](#)). The 90% dissolved subsamples are older, ranging from 37,740 ± 190 to 31,520 ± 100 $^{14}$C yr BP. For the most part, the ages increase with increasing dissolution of the outer part, except for shell 23GRØm-06-3 ([Fig. 2](#)). Calibrated and reservoir corrected using Marine20 (Heaton et al., [2020](#)) (and ΔR = 0), the ages on the 90% dissolved subsamples (median probability) range from 35,120 to 41,450 cal yr BP. We dated two additional shell fragments of *Astarte borealis* using a 90% dissolution; these are 27,870 ± 120 and 26,590 ± 130 $^{14}$C yr BP. We also calibrated and reservoir corrected the radiocarbon ages reported in Weidick et al. ([1996](#); Supplementary Table 1, shells treated with 50% leach; Håkansson,
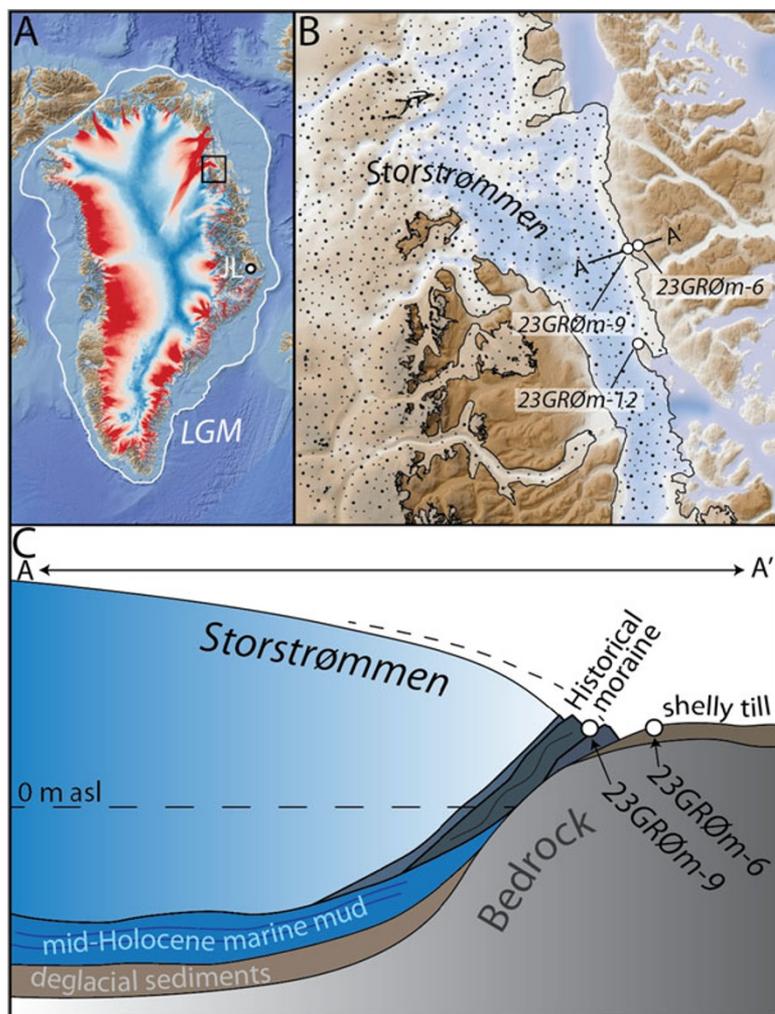
**Figure 1.** (**A**) The Greenland ice sheet today (showing velocity pattern: blue/red = low/high surface velocity) and at the last glacial maximum (LGM) (Sbarra et al., 2022). Small black box shows area of **B**; JL, Jameson Land. (**B**) Storstrømmen outlet glacier in NE Greenland (stippled pattern) showing topography/bathymetry (Morlighem et al., 2017), sample sites, and topographic cross section shown in **C**. (**C**) Cross section of Storstrømmen in area of sampling.
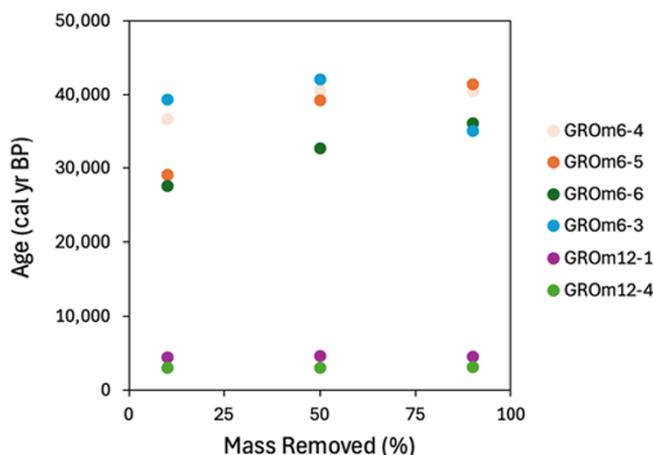


**Figure 2.** Radiocarbon ages of four shells from the till site (23GRØm-06) and two from the historical moraine (23GRØm-12) as a function of mass dissolved before dating.

K., personal communication, 2024), which range in age (median probability) from 28,250 to 37,110 cal yr BP.

Radiocarbon ages were obtained from two *Mya truncata* bivalve shells from the historical moraine (23GRØm-12). The 10% and 90% dissolved subsamples for one shell are 4490 ± 90 and 4540 ± 90 $^{14}$C yr BP, respectively; and the 10% and 90% dissolved subsamples of the second shell are 3360 ± 80 and 3430 ± 90 $^{14}$C yr BP, respectively (Fig. 2; Table 1). The radiocarbon ages of the differentially dissolved fragments overlap for the two Holocene shells.

**Table 1.** Radiocarbon ages on shells from the Storstrømmen region

| Lab ID (ACE)[a] | Sample ID | Taxon | Method[b] | Mass dissolved (%) | $^{14}$C age (BP) | ± | Cal yr BP (95% range) | Median probability[c] |
|---|---|---|---|---|---|---|---|---|
| Till site | | | | | | | | |
| 6899.1.1 | 23GRØm-06-4 | *Mya truncata* | AGE3 graphite | 10 | 33,100 | 118 | 37,090–36,381 | 36,749 |
| 6900.1.1 | 23GRØm-06-4 | *Mya truncata* | AGE3 graphite | 50 | 36,492 | 162 | 40,903–40,172 | 40,551 |
| 6901.1.1 | 23GRØm-06-4 | *Mya truncata* | AGE3 graphite | 90 | 36,450 | 168 | 40,877–40,116 | 40,515 |
| 6902.1.1 | 23GRØm-06-5 | *Mya truncata* | AGE3 graphite | 10 | 25,710 | 65 | 29,260–28,804 | 29,053 |
| 6903.1.1 | 23GRØm-06-5 | *Mya truncata* | AGE3 graphite | 50 | 35,065 | 143 | 39,602–39,000 | 39,296 |
| 6904.1.1 | 23GRØm-06-5 | *Mya truncata* | AGE3 graphite | 90 | 37,744 | 194 | 41,785–41,126 | 41,451 |
| 6905.1.1 | 23GRØm-06-6 | *Mya truncata* | AGE3 graphite | 10 | 24,212 | 56 | 27,720–27,312 | 27,528 |
| 6906.1.1 | 23GRØm-06-6 | *Mya truncata* | AGE3 graphite | 50 | 29,164 | 84 | 33,027–32,189 | 32,652 |
| 6907.1.1 | 23GRØm-06-6 | *Mya truncata* | AGE3 graphite | 90 | 32,531 | 113 | 36,437–35,870 | 36,153 |
| 6908.1.1 | 23GRØm-06-3 | *Mya truncata* | AGE3 graphite | 10 | 35,126 | 148 | 39,656–39,045 | 39,343 |
| 6909.1.1 | 23GRØm-06-3 | *Mya truncata* | AGE3 graphite | 50 | 38,947 | 210 | 42,322–41,874 | 42,106 |
| 6910.1.1 | 23GRØm-06-3 | *Mya truncata* | AGE3 graphite | 90 | 31,515 | 104 | 35,392–34,766 | 35,120 |
| 8280.1.1 | 23GRØm-06-1 | *Astarte borealis* | AGE3 graphite | 90 | 27,873 | 124 | 31,382–30,872 | 31,106 |
| 8281.1.1 | 23GRØm-06-2 | *Astarte borealis* | AGE3 graphite | 90 | 26,591 | 125 | 30,246–29,682 | 29,966 |
| Historical moraine | | | | | | | | |
| 6618.1.1 | 23GRØm-12-1 | *Mya truncata* | CHS GIS | 10 | 4494 | 87 | 4783–4225 | 4487 |
| 6619.1.1 | 23GRØm-12-1 | *Mya truncata* | CHS GIS | 50 | 4631 | 89 | 4911–4389 | 4657 |
| 6620.1.1 | 23GRØm-12-1 | *Mya truncata* | CHS GIS | 90 | 4538 | 88 | 4814–4282 | 4545 |
| 8279.1.1 | 23GRØm-12-1 | *Mya truncata* | AGE3 graphite | 90 | 4567 | 15 | 4767–4423 | 4582 |
| 6621.1.2 | 23GRØm-12-4 | *Mya truncata* | CHS GIS | 10 | 3364 | 79 | 3287–2796 | 3042 |
| 6622.1.1 | 23GRØm-12-4 | *Mya truncata* | CHS GIS | 50 | 3357 | 87 | 3290–2778 | 3034 |
| 6623.1.1 | 23GRØm-12-4 | *Mya truncata* | CHS GIS | 90 | 3426 | 88 | 3366–2856 | 3119 |

[a]Arizona Climate and Ecosystems (ACE) Isotope Laboratory, Northern Arizona University, Flagstaff, AZ.
[b]AGE3 graphite: graphite target generated from combustion using Automated Graphitization Equipment; CHS GIS: Carbonate Handling System with Gas Ion Source.
[c]Median of the calibrated age probability distribution using the marine20 calibration dataset (Heaton et al., 2020) and assumed ΔR = 0 yr.

The results of amino acid measurements on each shell, including the D/L values and concentrations from multiple amino acids, are provided in Supplementary Table 2. For this study, we focused on aspartic acid (Asp), which is among the most abundant amino acids in molluscan protein and is the best resolved chromatographically with our procedure (Kaufman and Manley, 1998). Asp may include a small component of asparagine, which was converted to Asp during laboratory hydrolysis.

Asp D/L values of the 18 shells from the till site generally agree, with most falling in the range of 0.30 and 0.40 (Supplementary Table 2). D/L values vary depending to some degree on taxon and the anatomical position of the shell that was sampled. Asp D/L values of the flank position (the thinner parts of the shell away from the umbo) of *Mya* shell fragments were distinctly higher (0.421 ± 0.008, n = 3) than others. We therefore focus on the results from the seven *Mya* shells that were sampled in their umbo area, which average 0.344 ± 0.034 ( ). Asp D/L values of the 20 *Mya* shells from the two historical moraines range from 0.127 to 0.179 (Supplementary Table 2), averaging 0.142 ± 0.013. And Asp D/L values of the nine known *Mya* shells from two last interglacial sites on Jameson Land range from 0.242 to 0.341 (Supplementary Table 2), and average

0.264 ± 0.039. The average Asp D/L values are summarized by site in Table 2.

## DISCUSSION

### AAR geochronology and paleothermometry

The extent of racemization in amino acids preserved in shells depends on both the shell age and its overall temperature history following deposition. More specifically, the rate of AAR as measured by the ratio of D to L enantiomers (D/L) is controlled by the effective diagenetic temperature ($T_{\text{eff}}$), which represents the integrated effect of changing temperature on the rate of racemization since the death of the organism. Like other chemical reactions, the temperature dependence of racemization can be modeled using the Arrhenius equation. For this procedure, modern samples are heated in the laboratory at different temperatures to measure the forward reaction rate, and Late Holocene samples whose ages are known from radiocarbon dating are used to estimate the reaction rate at ambient temperatures (e.g., Kaufman, 2006). The temperature sensitivity of Asp racemization in *Mya truncata* has already

**Table 2.** Extent of aspartic acid racemization (Asp D/L) in *Mya truncata* shells from East Greenland

| Lab ID (UAL)[a] | Field ID | Region | Deposit | Asp D/L | ± | n | Age (ka) | Age reference |
|---|---|---|---|---|---|---|---|---|
| 24314–24320 | 23GRØm-06 | Storstrømmen | Till site | 0.344 | 0.034 | 7 | 38.3[a] | Table 2 |
| 24304–24313 | 23GRØm-09 | Storstrømmen | Historical moraine | 0.137 | 0.008 | 10 | — | — |
| 24294–24303 | 23GRØm-12 | Storstrømmen | Historical moraine | 0.148 | 0.015 | 10 | 4.5, 3.1 | Table 2 |
| 24392–24396 | 82106 | Jameson Land | LIG site 96 | 0.254 | 0.049 | 5 | 125 ± 10 | Landvik et al. (1994) |
| 24397–24400 | 82110 | Jameson Land | LIG site 77 | 0.277 | 0.017 | 4 | 121 ± 10 | Vosgerau et al. (1994) |
| 24401–24403 | 82302 | Jameson Land | LIG site 97 | 0.345 | 0.070 | 3 | 192 ± 20 | Landvik et al. (1994) |

[a]UAL is the sample ID used in the Northern Arizona University Amino Acid Geochronology Laboratory.
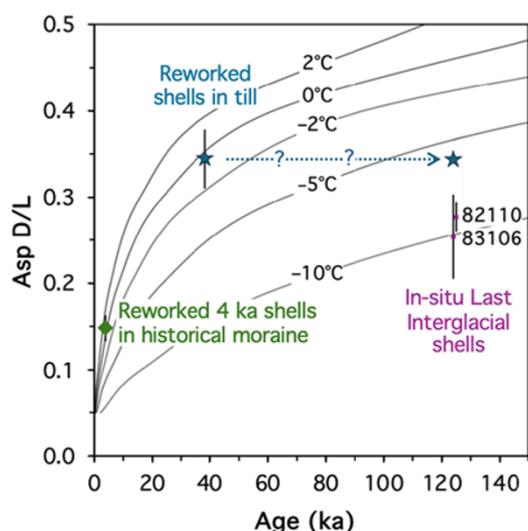[b]Average apparent age of 90%-dissolved subsamples from four shells.



**Figure 3.** Relation between the extent of aspartic acid racemization (Asp D/L) and shell age based on kinetic equations for *Mya truncata* under isothermal conditions and solved for five different effective diagenetic temperatures ($T_{eff}$) (Manley et al., 2000). Symbols show the average D/L values with ±1 SD uncertainties measured in shells from multiple collections. The shells collected from last glacial maximum (LGM) till are plotted according to their average $^{14}$C age of the 90% dissolved subsamples, but the correct age is more likely MIS 5e or older.

been quantified in this way (Manley et al., 2000; Fig. 3). While these published kinetic equations have important uncertainties due to varying diagenetic conditions, they can be used to approximate the postdepositional temperature history of the Greenland shells, assuming that the $^{14}$C ages are correct. We can then assess the reliability of the $^{14}$C age by evaluating whether the inferred temperature history is feasible, and we can evaluate the likelihood of alternative age–temperature combinations.

*Reworked shells in historical moraines*
Radiocarbon measured in two *Mya truncata* shells collected from a historical moraine (23GRØm-12) at Storstrømmen returned ages of 3.1 and 4.5 cal ka (90% dissolved; Table 1). We consider these ages to be reliable, because three differentially dissolved subsamples from each shell yielded overlapping ages. These roughly 4 cal ka marine shells were transported onshore and redeposited into the historical moraine by advancing Storstrømmen ice during the Little Ice Age (1450–1900 CE; Grove, 2001). Asp D/L values of 10 *Mya truncata* shells collected from the same moraine average 0.148 ± 0.015 (Table 2). Applying the mean Asp D/L value and an age of 4 cal ka to the kinetic equation of Manley et al. (2000) yields

a $T_{eff}$ of 0.5°C. This temperature is much higher than the recent mean annual temperature of −12°C at Danmarkshavn, the nearest meteorological station (https://www.climate.top/greenland/danmarkshavn/temperatures). However, the high temperature is reasonable for shells that resided under marine water or under warm-based glacial ice for essentially all their postdepositional history. Another collection of 10 *Mya truncata* shells from a second historical moraine (23GRØm-09) at Storstrømmen yielded a slightly lower average D/L value of 0.137 ± 0.008, which overlaps at ±1 SD with shells from the first site (Table 2). None of the shells from this site were analyzed for radiocarbon.

*Reworked shells in till*
Radiocarbon measured in four *Mya truncata* shells collected from till deposited near Storstrømmen (23GRØm-06) returned ages ranging from 35.1 to 41.5 cal ka (90% dissolved; Table 1). We distrust these ages, because the shell interiors yielded older ages than their exteriors, indicating a system open to exchanging carbon with the surrounding environment. Nonetheless, assuming that the midpoint age of 38 cal ka is correct, and applying the mean Asp D/L value of 0.344 (n = 7 shell beaks) to the kinetic equation of Manley et al. (2000) yields a $T_{eff}$ of −0.2°C. This temperature is similar to the one calculated for the 4 cal ka shells (discussed earlier) and would be reasonable if the shells were held under marine water or warm-based ice for nearly all their postdepositional history. However, we argue that this relatively high-temperature postdepositional history is unlikely. During the past 8000 yr or more since deglaciation (Weidick et al., 1996), the shells experienced a mean annual temperature approximated by the current mean annual temperature in the region (−12°C at Danmarkshavn). Additionally, during maximum ice phases (e.g., last glacial maximum [LGM]), this area could have been beneath cold-based ice. Landvik (1994) described highly weathered bedrock features across Germania Land that later research depicted to be within the LGM ice extent (Leger et al., 2024). The presence of weathered bedrock surfaces within LGM ice extent is common throughout the Arctic and is interpreted as occupation by cold-based ice (Briner et al., 2003; Gjermundsen et al., 2015; Beel et al., 2016). Cosmogenic nuclide measurements in Germania Land support the presence of cold-bedded conditions in the region (Skov et al., 2020). Thus, a low-temperature history that includes a substantial length of time at temperatures consistent with polar terrestrial ground and cold-based ice (i.e., −10°C to −20°C) is perhaps more likely. Assuming that the reworked shells from the till site date to MIS 5e (125 ka) indicates a $T_{eff}$ of −6°C (Fig. 3), which implies a temperature history that includes a period during which the shells were covered by marine water and/or warm-based ice. Regardless of the temperature history, the Asp D/L values of the reworked shells are higher than those of last

interglacial shells from Jameson Land (see next section), suggesting that the reworked shells are even older. In sum, the relatively high Asp D/L values in the reworked shells together with reasonable assumptions about the temperature history indicate that the shells date from MIS 5 or older.

### Last interglacial shells from Jameson Land

We measured the extent of AAR in shells that were previously collected from the well-studied Langelandselv succession on coastal Jameson Land (Landvik et al., 1994; Vosgerau et al., 1994). The shells are from marine deposits with luminescence ages and faunal elements that assign them to the last interglacial (Eemian, MIS 5e). Shells from the same collections were analyzed previously using ion-exchange chromatography, which only resolves the diastereomers of the slowly racemizing amino acid isoleucine (Rögnvaldsson and Sejrup, 1992). Here, we focus on Asp, which racemizes more rapidly and therefore affords a high-resolution chronometer at polar sites where the rate of AAR is low (Goodfriend et al., 1996). Collections of four or five individual *Mya truncata* shells were analyzed from each of two sites (Supplementary Table 2). The average D/L values are 0.254 ± 0.049 and 0.277 ± 0.017, and they overlap within their ±1 SD uncertainties (Fig. 3; Table 2). Assuming an age of 125 ka and applying the midpoint Asp D/L value (0.266) to the kinetic equation of Manley et al. (2000) yields a $T_{eff}$ of −9.5°C. This compares with a mean annual temperature of −7°C at Ittoqqortoormiit (https://www.climate.top/greenland/ittoqqortoormiit), located about 50 km east of the Langelandselv exposures. The −9.5°C $T_{eff}$ seems reasonable, considering the shells likely experienced temperatures that were both warmer (submarine and warm-based ice) and colder (glacial periods with ice-free conditions or cold-based ice cover) than recent air temperatures. A third collection of shells was analyzed from the deposit where Landvik et al. (1994) reported a luminescence age of 192 ± 20 ka. It yielded an Asp D/L value of 0.345 ± 0.070 (Table 2) consistent with an age older than MIS 5.

### Summary of amino acid geochronology

The Asp D/L values of shells collected from till at Storstrømmen are somewhat higher than those from known MIS 5e beds at Jameson Land. Considering that mean annual air temperature is about 5°C warmer at Jameson Land, we conclude that the Storstrømmen shells date from MIS 5e or older. These shells yielded finite $^{14}$C ages, with subsamples that are progressively younger toward the shell exterior and are therefore likely contaminated by young carbon. In contrast, the $^{14}$C ages of increasingly dissolved subsamples of shells incorporated into a historical moraine overlap, indicating that their ages (∼4 cal ka) are correct. Combining their average Asp D/L value and $^{14}$C age with the AAR kinetic equations (Manley et al., 2000) indicates that these shells experienced postdepositional temperatures consistent with submarine and sub–warm based ice. Temperatures this high are unlikely for the shells in the till, however, because they at least experienced the past ∼8000 yr at present-day air temperatures of −12°C and subzero temperatures for at least portions of past cold-based ice cover.

### Radiocarbon dating old shells in northern Greenland

The interpretation that the bivalve shells from the till site date from before MIS 3 indicates that they are too deeply contaminated with young carbon to yield reliable radiocarbon ages. The younger $^{14}$C ages of the two *Astarte* shells imply a greater degree of contamination than for the *Mya* shells (Table 1), indicating that shell type can

play a role. Even trace amounts of contamination of a radiocarbon-dead shell by young carbon can lead to finite (MIS 3) ages (Olsson, 2009; Rech et al., 2011). For example, the apparent $^{14}$C age of a radiocarbon-dead shell contaminated by just 0.5% modern carbon ($F_m = 1$) would be 42.6 ka. In contrast, the apparent age of a 4.1 ka shell contaminated by the same proportion of modern carbon would shift undetectably by only 27 yr. Our finding is consistent with prior literature; in particular, Busschers et al. (2014) investigated sources of contamination in shells and found considerable amounts of a secondary carbonate precipitate that they attribute to a bacterial origin.

Is it possible that contamination has compromised previously reported MIS 3 ages from across northern Greenland? Eight shells dated by Larsen et al. (2018) from ground moraine beyond the historical ice-sheet limit on Lambert Land, Northeast Greenland, range in age from 24.4 to 37.1 cal ka. The samples, treated by removing 25% of their mass before dating, are *Hiatella arctica, Mya truncata*, and fragments identified as snail and "suspension feeder." These results were combined with those previously reported from our till site by Weidick et al. (1996) and used to suggest that the Northeast Greenland Ice Stream was smaller during MIS 3 than it was during the historical period. Six shells (*Hiatella arctica* and *Astarte borealis*) dated by Larsen et al. (2019) from the historical moraine of a northern outlet of Flade Isblink, Northeast Greenland, range from 39.8 to 52.4 cal ka. The shells received a 15% leach, leading Larsen et al. (2019) to interpret them as reliable and dating to MIS 3, indicating that Flade Isblink was smaller during that time than at present. Finally, 12 shells (*Hiatella arctica* and *Mya truncata*) dated by Søndergaard et al. (2019) from ground moraine ∼15 km beyond the historical ice limit of the Greenland Ice Sheet in Northwest Greenland yielded MIS 3 radiocarbon ages. The shells, treated with an unspecified amount of leaching, range from 26.8 to 38.4 cal ka and were interpreted as evidence to support a Greenland Ice Sheet smaller during MIS 3 than today's extent. Based on our results, we think it unlikely that the northern Greenland Ice Sheet was smaller during MIS 3 than it is at present, and instead that these previously dated shells may be contaminated.

We next explore the likelihood of finding old shells in young sediments more broadly across northern Greenland. A compilation of radiocarbon-dated bivalves from Greenland (Sinclair et al., 2016) shows many pre-Holocene finite ages, especially in parts of Greenland adjacent to present-day cold-based ice (MacGregor et al., 2022), largely in northern Greenland (Fig. 4). These may be areas that receive only light to no subglacial erosion under mostly frozen bedded conditions when the Greenland Ice Sheet is in stadial or glacial modes, resulting in the preservation of interglacial sediment formations (Feyling-Hanssen et al., 1983; Funder and Símonarson, 1984; Hjort and Feyling-Hanssen, 1987; Bennike et al., 1994, 2002, 2010; Kelly et al., 1999; Funder et al., 2001). Such sediment packages are a source of entrainment of fossiliferous sediments into overriding ice. Following deposition, these radiocarbon-nonfinite bivalve shells sourced from ancient sediment sequences are then sometimes contaminated, perhaps once they are eroded to and then reside near the surface.

### Supporting evidence for Greenland Ice Sheet size during MIS 3

Some existing ice-sheet and climate records spanning the last glacial cycle are inconsistent with a Greenland Ice Sheet smaller than at present during MIS 3. The dust record from the Renland Ice Cap, in central East Greenland, has been used to suggest that ice-sheet recession during MIS 5e was comparable to that of the
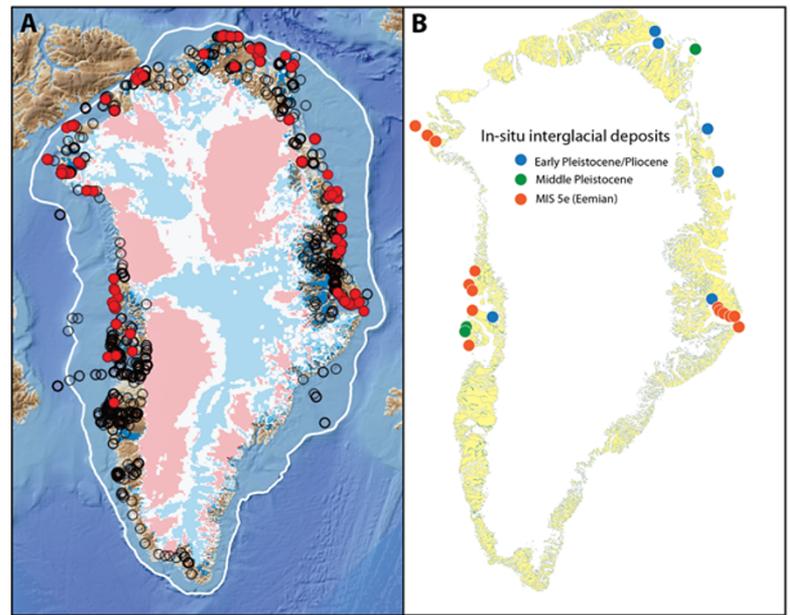
**Figure 4.** (**A**) Map of Greenland showing last glacial maximum (LGM) ice extent (white line) and modeled basal thermal state (red = thawed, blue = frozen, gray = uncertain; MacGregor et al., 2022). Circles show radiocarbon age compilation from Sinclair et al. (2016); ages on shells >15 ka, a time when all of Greenland was covered by ice, shown in red. (**B**) Locations of pre-Holocene in situ sediment sections (Feyling-Hanssen et al., 1983; Funder and Símonarson, 1984; Hjort and Feyling-Hanssen, 1987; Bennike et al., 1994, 2002, 2010; Kelly et al., 1999; Funder et al., 2001).

Holocene, and that only minor amounts of ice-free land may have existed between the two interglaciations (Simonsen et al., 2019). Greenland ice-core records suggest that although climate was oscillating during MIS 3, baseline climate conditions were more glacial than interglacial (Kindler et al., 2014), a finding similarly revealed by pollen records in northwest Europe (Guiter et al., 2003). An additional ice-core proxy for interglacial-level warmth is melt layers and impacts of melting on ice constituents like methane. Although melt layers are documented in ice cores during the Holocene (Herron et al., 1981; Alley and Anandakrishnan, 1995; Westhoff et al., 2021) and MIS 5e (NEEM Community Members, 2013), there is no evidence for melt layers in intervening periods, including during MIS 3 (Chappelaz et al., 2013). Foraminifera and ice-rafted debris data from the northern North Atlantic typically show stadial conditions during MIS 3 that are more glacial than interglacial when compared with sediments from MIS 5 and 1 (e.g., Bauch et al., 2012).

The formation of Heinrich and Baffin-Bay Detrital Carbonate (BBDC) layers are typically interpreted as requiring glaciation onto continental shelves, perhaps involving the dynamics of expansive ice shelves like that recently highlighted in Baffin Bay (Couette et al., 2022; Batchelor et al., 2024). Several Heinrich and BBDC layers occur during MIS 3, indicating that the Laurentide and Greenland Ice Sheets extended onto their continental shelves during at least several discrete time periods during MIS 3 (Simon et al., 2014; Jackson et al., 2023; Fig. 5). However, there is a >5 ka gap between H4 and H5 with no BBDC event that could involve a reduced ice sheet; similarly, there are two brief episodes (~35 ka and ~52 ka) with notable decreases in West Greenland Ice Sheet–sourced sediments in Baffin Bay (Fig. 5). The shell radiocarbon data, on the other hand, when taken together and at face value, span times of Heinrich and BBDC activity, making significant ice-sheet recession at these particular times seem unlikely.

Some existing paleoclimate records of MIS 3 conditions, however, possibly could be compatible with short-lived episodes of significant Greenland Ice Sheet recession. For example, some MIS 3 sites in Scandinavia record mild conditions. Wohlfarth et al. (2011) documented an Arctic to sub-Arctic environment with July

temperatures of 8–14°C from ~50 to ~40 ka in central Sweden (using microfossil and macrofossil data) where recent July temperatures are ~14°C (https://www.climate.top/sweden/ostersund). In northern Finland, Helmens et al. (2018) reconstructed July temperatures during MIS 3 that were similar to present-day based on extensive multiproxy paleoecological data. At another site in northern Finland, Sarala et al. (2016) reported paleobotanical evidence for July temperatures during late MIS 3 that might have been even higher than present-day temperatures. Mangerud et al. (2008) found evidence for sub-Arctic mollusks living along the coast of the Arctic island Novaya Zemlya during MIS 3. Additional evidence for MIS 3 summer temperatures similar to present-day temperatures in Beringia and Siberia, largely inferred from pollen studies, is summarized by Miller et al. (2010). These mild conditions may relate to Holocene-like warmth of intermediate water in the Arctic Ocean during MIS 3 (Cronin et al., 2012). Larsen et al. (2018) reconstruct a Northeast Greenland Ice Sheet that was smaller from 41 to 26 ka than at present and infer that MIS 3 summers were 6–8°C warmer than the LGM yet still 8–12°C colder than the preindustrial period. They attributed to warmth to the unusually high orbital precession index around that time and wondered if this temperature combined with a significant reduction in snowfall accumulation rate could result in a rather limited Greenland Ice Sheet extent during MIS 3.

Tabone et al. (2019) simulated the ice sheet in Northeast Greenland in an attempt to match the MIS 3 reconstruction implied by Larsen et al.'s (2018) reconstruction. They argued that because ice core–inferred atmospheric temperatures may be unlikely to drive such a recession, it may be possible to do so with ocean thermal forcing. Although Tabone et al. (2019) could simulate significant recession from a previously extensive ice position with significant ocean thermal forcing, the simulated ice margin never reached a position smaller than today's.

To summarize, the bulk of supporting evidence, including ice-core temperature reconstructions, ice-core dust, ice-core melt layers, temperature proxy data from Europe, and ice-rafted debris studies in Baffin Bay, is lacking support for a Holocene-sized Greenland Ice Sheet during MIS 3. If such an ice configuration
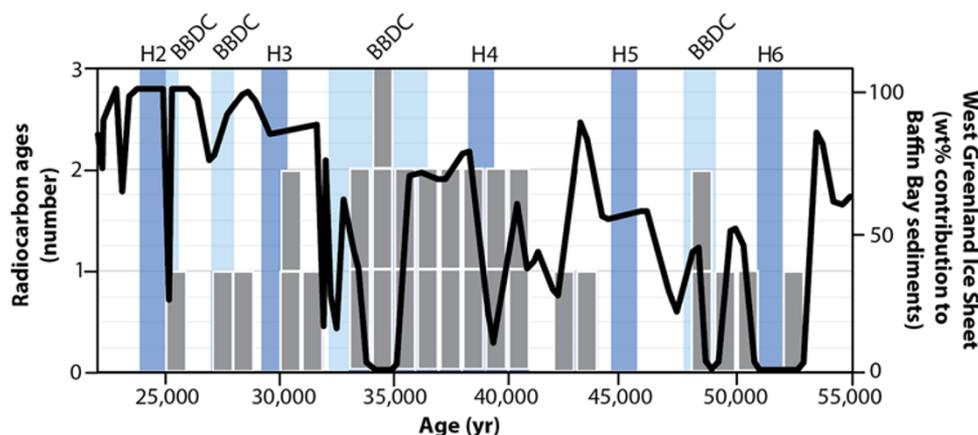
**Figure 5.** Histogram showing previously published reworked bivalve shell fragment ages (references listed in Supplementary Table 1) and the 90% shell-dissolved ages reported here (Table 1). Solid black line is the abundance (weight percent) of Uummannaq-sourced mineral grains in a Baffin Bay sediment core, with higher values interpreted as more extensive Uummannaq ice streams (Simon et al., 2014). The timing of Heinrich Events (H#) and Baffin Bay Detrital Carbonate (BBDC) events are shown as dark blue and light blue bars, respectively (from Simon et al., 2014). The interpretation that the Greenland Ice Sheet was smaller than present during the times implied by the radiocarbon ages is at odds with the occurrence of Heinrich Events and BBDCs, which seem to require ice-sheet expansion to the edge of the continental shelf.

was achieved, it would almost certainly have involved ocean forcing to remove grounded ice positions on Greenland's continental shelves and potentially as far inland as the ice is today. Available data allow for such a configuration only for brief (few thousands of years maximum) windows of time and most likely not from 41 to 26 ka (Larsen et al., 2018).

## Conclusion

Prior work has shown that radiocarbon-nonfinite bivalve shells, with even minor contamination by young carbon, can yield finite radiocarbon ages that date to MIS 3. Thus, MIS 3–aged reworked bivalve shells reported from North Greenland could be similarly affected by contamination, which would be more consistent with inferences of Greenland Ice Sheet size based on existing records of climate, global ice volume, and sea level. Our resampling of an MIS 3 shell site at Storstrømmen yielded MIS 3 radiocarbon ages that generally increase in age with increasing dissolution. Our amino acid results suggest that these shells date to MIS 5e or older. On the other hand, ocean thermal forcing during MIS 3 is unknown, and interstadial spikes of mild summer temperature (during times with high precession index) combined with accumulation rates that were much lower than during the Holocene could have led to episodes of short-lived ice-sheet recession. Ultimately, more work is required to more fully test the hypothesis that the Greenland Ice Sheet was smaller during MIS 3 than it is today. Such investigations could focus on ice-sheet modeling, expanding amino acid data generation, and more rigorous radiocarbon dating.

## References

Alley, R.B., Anandakrishnan, S., 1995. Variations in melt-layer frequency in the GISP2 ice core: implications for Holocene summer temperatures in central Greenland. *Annals of Glaciology* **21**, 64–70.

Bard, E., Tuna, T., Fagault, Y., Bonvalot, L., Wacker, L., Fahrni, S., Synal, S., 2015. AixMICADAS, the accelerator mass spectrometer dedicated to ¹⁴C recently installed in Aix-en-Provence, France. *Nuclear Instruments and Methods in Physics Research Section B: Beam Interactions with Materials and Atoms* **361**, 80–86.

Batchelor, C.L., Krawczyk, D.W., O'Brien, E., Mulder, J., 2024. Shelf-break glaciation and an extensive ice shelf beyond northwest Greenland at the Last Glacial Maximum. *Marine Geology* **476**, 107375.

Batchelor, C.L., Margold, M., Krapp, M., Murton, D.K., Dalton, A.S., Gibbard, P.L., Stokes, C.R., Murton, J.B., Manica, A., 2019. The configuration of Northern Hemisphere ice sheets through the Quaternary. *Nature Communications* **10**, 3713.

Bauch, H.A., Kandiano, E.S., Helmke, J.P., 2012. Contrasting ocean changes between the subpolar and polar North Atlantic during the past 135 ka. *Geophysical Research Letters* 39. https://doi.org/10.1029/2012GL051800.

Bednarski, J., 1995. Glacial advances and stratigraphy in Otto Fiord and adjacent areas, Ellesmere Island, Northwest Territories. *Canadian Journal of Earth Sciences* **32**, 52–64.

Beel, C.R., Lifton, N.A., Briner, J.P., Goehring, B.M., 2016. Quaternary evolution and ice sheet history of contrasting landscapes in Uummannaq and Sukkertoppen, western Greenland. *Quaternary Science Reviews* **149**, 248–258.

Bennike, O., Abrahamsen, N., Malgorzata, B., Israelson, C., Konradi, P., Matthiessen, J., Witkowski, A., 2002. A multi-proxy study of Pliocene sediments from Île de France, North-East Greenland. *Palaeogeography, Palaeoclimatology, Palaeoecology* **186**, 1–23.

Bennike, O., Böcher, J., 1994. Land biotas of the last interglacial/glacial cycle on Jameson Land, East Greenland. *Boreas* **23**, 479–487.

Bennike, O., Hansen, K.B., Knudsen, K.L., Penney, D.N., Rasmussen, K.L., 1994. Quaternary marine stratigraphy and geochronology in central West Greenland. *Boreas* **23**, 194–215.

Bennike, O., Knudsen, K.L., Abrahamsen, N., Böcher, J., Cremer, H., Wagner, B., 2010. Early Pleistocene sediments on Store Koldewey, northeast Greenland. *Boreas* **39**, 603–619.

Bright, J., Ebert, C., Flores, C., Harnik, P.G., Huntley, J.W., Kowalewski, M., Portell, R.W., Retelle, M., Schuur, E.A., Kaufman, D.S., 2024. Comparing MICADAS gas source, direct carbonate, and standard graphite ¹⁴C determinations of biogenic carbonate. *Radiocarbon* **66**, 295–305.

Briner, J.P., Miller, G.H., Davis, P.T., Bierman, P.R., Caffee, M., 2003. Last Glacial Maximum ice sheet dynamics in arctic Canada inferred from young erratics perched on ancient tors. *Quaternary Science Reviews* **22**, 437–444.

Burr, G.S., Edwards, R.L.. Donahue, D.J., Druffel, E.R.M., Taylor, F.W., 1992. Mass spectrometric $^{14}$C and U-Th measurements in coral. *Radiocarbon* **34**, 611–618.

Busschers, F.S., Wesselingh, F.P., Kars, R.H., Versluijs-Helder, M., Wallinga, J., Bosch, J.H.A., Timmner, J., *et al*, 2014. Radiocarbon dating of Late Pleistocene marine shells from the southern North Sea. *Radiocarbon* **56**, 1151–1166.

Chappellaz, J., Stowasser, C., Blunier, T., Baslev-Clausen, D., Brook, E.J., Dallmayr, R., Faïn, X., *et al*, 2013. High-resolution glacial and deglacial record of atmospheric methane by continuous-flow and laser spectrometer analysis along the NEEM ice core. *Climate of the Past* **9**, 2579–2593.

Clark, P.U., Shakun, J.D., Rosenthal, Y., Köhler, P., Bartlein, P.J., 2024. Global and regional temperature change over the past 4.5 million years. *Science* **383**, 884–890.

Couette, P.-O., Lajeunesse, P., Ghienne, J.-F., Dorschel, B., Gebhardt, C., Hebbeln, D., Brouard, E., 2022. Evidence for an extensive ice shelf in northern Baffin Bay during the Last Glacial Maximum. *Communications Earth & Environment* **3**, 1–12.

Cronin, T.M., Dwyer, G.S., Farmer, J., Bauch, H.A., Spielhagen, R.F., Jakobsson, M., Nilsson, J., Briggs W.M, Stepanova, A., 2012. Deep Arctic Ocean warming during the last glacial cycle. *Nature Geoscience* **5**, 631–634

Dalton, A.S., Finkelstein, S.A., Forman, S.L., Barnett, P.J., Pico, T., Mitrovica, J.X., 2019. Was the Laurentide Ice Sheet significantly reduced during Marine Isotope Stage 3? *Geology* **47**, 111–114.

Dalton, A.S., Stokes, C.R., Batchelor, C.L., 2022. Evolution of the Laurentide and Innuitian ice sheets prior to the Last Glacial Maximum (115 ka to 25 ka). *Earth-Science Reviews* **224**, 103875.

Dumitru, O.A., Dyer, B., Austermann, J., Sandstrom, M.R., Goldstein, S.L., D'Andrea, W.J., Cashman, M., Creel, R., Bolge, L., Raymo, M.E., 2023. Last interglacial global mean sea level from high-precision U-series ages of Bahamian fossil coral reefs. *Quaternary Science Reviews* **318**, 108287.

Farmer, J.R., Pico, T., Underwood, O.M., Cleveland Stout, R., Granger, J., Cronin, T.M., Fripiat, F., Martínez-García, A., Haug, G.H., Sigman, D.M., 2023. The Bering Strait was flooded 10,000 years before the Last Glacial Maximum. *Proceedings of the National Academy of Sciences USA* **120**, e2206742119.

Feyling-Hanssen, R.W., Funder, S., Petersen, K.S., 1983. The Lodin Elv Formation; a Plio-Pleistocene occurrence in Greenland. *Bulletin of the Geological Society of Denmark* **31**, 81–106.

Fox-Kemper, B., Hewitt, H.T., Xiao, C., Aðalgeirsdóttir, G., Drijfhout, S.S., Edwards, T.L., Golledge, N.R., *et al*, 2021. Ocean, Cryosphere and Sea Level Change. In Climate Change 2021: The Physical Science Basis. Contribution of Working Group I to the Sixth Assessment Report of the Intergovernmental Panel on Climate Change. Cambridge University Press, Cambridge, pp. 1211–1362.

Funder, S., Bennike, O., Böcher, J., Israelson, C., Petersen, K.S., Símonarson, L.A., 2001. Late Pliocene Greenland—the Kap København Formation in North Greenland. *Bulletin of the Geological Society of Denmark* **48**, 117–134.

Funder, S., Símonarson, L., 1984. Bio- and aminostratigraphy of some Quaternary marine deposits in West Greenland. *Canadian Journal of Earth Sciences* **21**, 843–852.

Gjermundsen, E.F., Briner, J.P., Akçar, N., Foros, J., Kubik, P.W., Salvigsen, O., Hormes, A., 2015. Minimal erosion of Arctic alpine topography during Late Quaternary glaciation. *Nature Geoscience* **8**, 789–792.

Goodfriend, G.A., Brigham-Grette, J., Miller, G.H., 1996. Enhanced age resolution of the marine Quaternary record in the Arctic using aspartic acid racemization dating of bivalve shells. *Quaternary Research* **45**, 176–187.

Gowan, E.., Zhang, X., Khosravi, S., Rovere, A., Stocchi, P., Hughes, A.L.C., Gyllencreutz, R., Mangerud, J., Svendsen, J.-I., Lohmann, G., 2021. A new global ice sheet reconstruction for the past 80 000 years." *Nature Communications* **12**, 1199.

Grove, J.M., 2001. The initiation of the "Little Ice Age" in regions round the North Atlantic. *Climatic Change* **48**, 53–82.

Guiter, F., Andrieu-Ponel, V., de Beaulieu, J.-L., Cheddadi, R., Calvez, M., Ponel, P., Reille, M., Keller, T., Goeury, C., 2003. The last climatic cycles in western Europe: a comparison between long continuous lacustrine sequences from France and other terrestrial records. *Quaternary International* **111**, 59–74.

Hajdas, I., Bonani, G., Herrgesell Zimmerman, S., Mendelson, M., Hemming, S., 2004. $^{14}$C ages of ostracodes from Pleistocene lake sediments of the Western Great Basin, Usa—results of progressive acid leaching." *Radiocarbon* **46**, 189–200.

Heaton, T.J., Köhler, P., Butzin, M., Bard, E., Reimer, R.W., Austin, W.E.N., Bronk Ramsey, C., *et al*, 2020. Marine20—The Marine Radiocarbon Age Calibration Curve (0–55,000 Cal BP). *Radiocarbon* **62**, 779–820.

Helmens, K.F., Katrantsiotis, C., Salonen, J.S., Shala, S., Bos, J.A.A., Engels, S., Kuosmanen, N., *et al*, 2018. Warm summers and rich biotic communities during N-hemisphere deglaciation. *Global and Planetary Change* **167**, 61–73.

Herron, M.M., Herron, S.L., Langway, C.C, 1981. Climatic signal of ice melt features in southern Greenland. *Nature* **293**, 389–391.

Hjort, C., Feyling-Hanssen, R.W., 1987. The Ymer-Formation—an interglacial sequence in northeasternmost Greenland. *Polar Research* **5**, 347–350.

Hodder, T.J., Gauthier, M.S., Ross, M., Lian, O.B., 2023. Was there a nonglacial episode in the western Hudson Bay Lowland during Marine Isotope Stage 3? *Quaternary Research* **116**, 148–161.

Jackson, R., Frederichs, T., Schulz, H., Kucera, M., 2023. Chronology of detrital carbonate events in Baffin Bay reveals different timing but similar average recurrence time of North American-Arctic and Laurentide ice sheet collapse events during MIS 3. *Earth and Planetary Science Letters* **613**, 118191.

Kaufman, D.S., 2006. Temperature sensitivity of aspartic and glutamic acid racemization in the foraminifera *Pulleniatina*. *Quaternary Geochronology* **1**, 188–207.

Kaufman, D.S., Manley, W.F., 1998. A new procedure for determining DL amino acid ratios in fossils using reverse phase liquid chromatography. *Quaternary Science Reviews* **17**, 987–1000.

Kelly, M., Funder, S., Houmark-Nielsen, M., Knudsen, K.L., Kronborg, C., Landvik, J., Sorby, L., 1999. Quaternary glacial and marine environmental history of northwest Greenland: a review and reappraisal. *Quaternary Science Reviews* **18**, 373–392.

Kindler, P., Guillevic, M., Baumgartner, M., Schwander, J., Landais, A., Leuenberger, M., 2014. Temperature reconstruction from 10 to 120 kyr b2k from the NGRIP ice core. *Climate of the Past* **10**, 887–902.

Kopp, R.E., Simons, F.J., Mitrovica, J.X., Maloof, A.C., Oppenheimer, M., 2013. A probabilistic assessment of sea level variations within the last interglacial stage. *Geophysical Journal International* **193**, 711–716.

Landvik, J.Y., 1994. The last glaciation of Germania Land and adjacent areas, northeast Greenland. *Journal of Quaternary Science* **9**, 81–92.

Landvik, J.Y., Lyså, A., Funder, S., Kelly, M., 1994. The Eemian and Weichselian stratigraphy of the Langelandselv area, Jameson Land, East Greenland. *Boreas* **23**, 412–423.

Larsen, N.K., Levy, L.B., Carlson, A.E., Buizert, C., Olsen, J., Strunk, A., Bjørk, A.A., Skov, D.S., 2018. Instability of the Northeast Greenland Ice Stream over the last 45,000 years. *Nature Communications* **9**, 1872.

Larsen, N.K., Levy, L.B., Strunk, A., Søndergaard, A.S., Olsen, J., Lauridsen, T.L., 2019. Local ice caps in Finderup Land, North Greenland, survived the Holocene Thermal Maximum. *Boreas* **48**, 551–562.

Leger, T.P.M., Clark, C.D., Huynh, C., Jones, S., Ely, J.C., Bradley, S.L., Diemont, C., Hughes, A.L.C., 2024. A Greenland-wide empirical reconstruction of paleo ice sheet retreat informed by ice extent markers: PaleoGrIS Version 1.0. *Climate of the Past* **20**, 701–755.

Lisiecki, L.E., Raymo, M.E., 2005. A Pliocene-Pleistocene stack of 57 globally distributed benthic $\delta^{18}$O records. *Paleoceanography* 20. https://doi.org/10.1029/2004PA001071.

MacGregor, J.A., Chu, W., Colgan, W.T., Fahnestock, M.A., Felikson, D., Karlsson, N.B., Nowicki, S.M.J., Studinger, M., 2022. GBaTSv2: a revised synthesis of the likely basal thermal state of the Greenland Ice Sheet. *The Cryosphere* **16**, 3033–3049.

Mangerud, J., Alexanderson, H., Birks, H.H., Paus, A., Perić, Z.M., Svendsen, J.I., 2023. Did the Eurasian ice sheets melt completely in early Marine Isotope Stage 3? New evidence from Norway and a synthesis for Eurasia. *Quaternary Science Reviews* **311**, 108136.

Mangerud, J., Kaufman, D., Hansen, J., Svendsen, J.I., 2008. Ice-free conditions in Novaya Zemlya 35 000-30 000 cal years B.P., as indicated by radiocarbon ages and amino acid racemization evidence from marine molluscs. *Polar Research* 27, 187–208.

Manley, W.F., Miller, G.H., Czywczynski, J., 2000. Kinetics of aspartic acid racemization in *Mya* and *Hiatella*: modelling age and paleotemperature of high-latitude Quaternary mollusks. In: Goodfriend, G.A., Collins, M.J., Fogel, M.L., Macko, S.A., Wehmiller, J.F. (eds.), *Perspectives in Amino Acid and Protein Geochemistry*. Oxford University Press, New York, pp. 202–218.

Miller, G.H., Andrews, J.T., 2019. Hudson Bay was not deglaciated during MIS-3. *Quaternary Science Reviews* 225, 105944.

Miller, G.H., Brigham-Grette, J., Alley, R.B., Anderson, L., Bauch, H.A., Douglas, M.S.V., Edwards, M.E., *et al*, 2010. Temperature and precipitation history of the Arctic. *Quaternary Science Reviews* 29, 1679–1715.

Morlighem, M., Williams, C.N., Rignot, E., An, L., Arndt, J.E., Bamber, J.L., Catania, G., *et al*, 2017. BedMachine v3: complete bed topography and ocean bathymetry mapping of Greenland from multibeam echo sounding combined with mass conservation. *Geophysical Research Letters* 44, 11051–11061.

NEEM Community Members, 2013. Eemian interglacial reconstructed from a Greenland folded ice core. *Nature* 493, 489–494.

Olsson, I.U., 2009. Radiocarbon dating history: early days, questions, and problems met. Radiocarbon 51, 1–43.

Pico, T., Creveling, J.R., Mitrovica, J.X., 2017. Sea-level records from the U.S. mid-Atlantic constrain Laurentide Ice Sheet extent during Marine Isotope Stage 3. *Nature Communications* 8, 15612.

Rech, J.A., Pigati, J.S., Lehmann, S.B., McGimpsey, C.N., Grimley, D.A., Nekola, J.C., 2011. Assessing open-system behavior of 14C in terrestrial gastropod shells. *Radiocarbon* 53,325–335.

Rögnvaldsson, F., Sejrup, H.P., 1992. Amino acid ratios in molluscs from raised marine deposits, Jameson Land, East Greenland. *Lundqua Report* 35, 215–224.

Sarala, P., Väliranta, M., Eskola, T., Vaikutiené, G., 2016. First physical evidence for forested environment in the Arctic during MIS 3. *Scientific Reports* 6, 29054.

Sbarra, C.M., Briner, J.P., Graham, B.L., Poinar, K., Thomas, E.K., Young, N.E., 2022. Evidence for a more extensive Greenland Ice Sheet in southwestern Greenland during the Last Glacial Maximum. *Geosphere* 18, 1316–1329.

Simon, Q., Hillaire-Marcel, C., St-Onge, G., Andrews, J.T., 2014. Northeastern Laurentide, western Greenland and southern Innuitian ice stream dynamics during the last glacial cycle. *Journal of Quaternary Science* 29, 14–26.

Simonsen, M.F., Baccolo, G., Blunier, T., Borunda, A., Delmonte, B., Frei, R., Goldstein, S., *et al*, 2019. East Greenland ice core dust record reveals timing of Greenland ice sheet advance and retreat. *Nature Communications* 10, 4494.

Sinclair, G., Carlson, A.E., Mix, A.C., Lecavalier, B.S., Milne, G., Mathias, A., Buizert, C., DeConto, R., 2016. Diachronous retreat of the Greenland ice sheet during the last deglaciation. *Quaternary Science Reviews* 145, 243–258.

Skov, D.S., Andersen, J.L., Olsen, J., Jacobsen, B.H., Knudsen, M.F., Jansen, J.D., Larsen, N.K., Egholm, D.L., 2020. Constraints from cosmogenic nuclides on the glaciation and erosion history of Dove Bugt, northeast Greenland. *GSA Bulletin* 132, 2282–2294.

Søndergaard, A.S., Larsen, N.K., Olsen, J., Strunk, A., Woodroffe, S., 2019. Glacial history of the Greenland Ice Sheet and a local ice cap in Qaanaaq, northwest Greenland. *Journal of Quaternary Science* 34, 536–547.

Synal, H.-A., Stocker, M., Suter, M., 2007. MICADAS: a new compact radiocarbon AMS system. *Nuclear Instruments and Methods in Physics Research B* 259, 7–13.

Tabone, I., Robinson, A., Alvarez-Solas, J., Montoya, M., 2019. Submarine melt as a potential trigger of the North East Greenland Ice Stream margin retreat during Marine Isotope Stage 3. *The Cryosphere* 13, 1911–1923.

Tierney, J.E., Poulsen, C.J., Montañez, I.P., Bhattacharya, T., Feng, R., Ford, H.L., Hönisch, B., *et al*, 2020. Past climates inform our future. *Science* 370, eaay3701.

Vosgerau, H., Funder, S., Kelly, M., Knudsen, K.L., Kronborg, C., Madsen, H.B., Sejrup, H.P., 1994. Palaeoenvironments and changes in relative sea level during the last interglaciation at Langelandselv, Jameson Land, East Greenland. *Boreas* 23, 398–411.

Wacker, L., Fahrni, S.M., Hajdas, I., Molnar, M., Synal, H.-A., Szidat, S., Zhang, Y.L., 2013. A versatile gas interface for routine radiocarbon analysis with a gas ion source. *Nuclear Instruments and Methods in Physics Research B* 294, 315–319.

Wehmiller, J.F., 1984. Interlaboratory comparison of amino acid enantiomeric ratios in fossil Pleistocene mollusks. *Quaternary Research* 22, 109–120.

Wehmiller, J.F., Miller, G.H., 2000. Aminostratigraphic dating methods in Quaternary geology. In: Noller J.S., Sowers, J.M., Lettis, W.R. (eds.), *Quaternary Geochronology*. AGU Reference Shelf Series 4. American Geophysical Union, Washington, DC, pp. 187–222.

Weidick, A., Andreasen, C., Oerter, H., Reeh, N., 1996. Neoglacial glacier changes around Storstrømmen, North-east Greenland. *Polarforschung* 64, 95–108.

Westhoff, J., Sinnl, G., Svensson, A., Freitag, J., Kjær, H.A., Vallelonga, P., Vinther, B., Kipfstuhl, S., Dahl-Jensen, D., Weikusat, I., 2021. Melt in the Greenland EastGRIP ice core reveals Holocene warming events. *Climate of the Past Discussions* 2021, 1–36

Wohlfarth, B., Alexanderson, H., Ampel, L., Bennike, O., Engels, S., Johnsen, T., Lundqvist, J., Reimer, P., 2011. Pilgrimstad revisited—a multi-proxy reconstruction of early/middle Weichselian climate and environment at a key site in central Sweden." *Boreas* 40, 211–230.